Evolution of graphene mediated magnetic coupling between Fe-chains

S. V. Ong, R. Robles, S. N. Khanna

Department of Physics, 701 W. Grace St., P.O. Box 842000, Virginia Commonwealth University, Richmond, VA 23284-2000, USA

Abstract

First principles electronic structure studies on the structure, stability, and magnetic coupling of Fe-chains at the zigzag edges of graphene ribbons have been carried out within a gradient-corrected density functional formalism. Our studies indicate that Fe sites in the chain undergo a structural rearrangement into Fe-Fe pairs. The Fe sites within a given chain are ferromagnetically aligned, but chains across the ribbon have an antiferromagnetic ground state. Studies on ribbons of increasing width show that the energy difference between magnetic states decreases with increasing width attaining a value of only 8.9 meV per unit cell for chains separated by 2 nm.

Keywords: Fe-chains, Graphene, Nano-Ribbons, Magnetic Coupling

1. Introduction

The possibility of experimentally isolating single sheets of graphene and investigating the electronic, magnetic, optical, and chemical behavior of this two-dimensional arrangement of carbon atoms has generated considerable excitement [1–5]. The single carbon sheet is a zero gap semiconductor, where the electrons behave like Dirac Fermions with linear energy dispersion and electron hole symmetry offering unusual transport properties [6].These include a display of quantum Hall effect at room temperature, ballistic transport at sub-micrometer scale, and finite conductivity at zero carrier concentrations [7]. These novel features are accompanied by developments in experimental techniques [8–13] allowing fabrication of graphene based nanostructures including ribbons, dots and graphene molecules and clusters. The properties of these nanostructures can be very different from those of graphene largely due to the surface and edges [11, 14–22]. For example, graphene ribbons have been found to be semiconducting with variable band gap or even metallic [23–26].

One of the properties that have drawn considerable attention is the possibility of localized magnetic moments associated with edges in graphene-based nanostructures. While bulk graphite is diamagnetic [27], the electron-electron interaction can stabilize magnetic moments at the edges in graphene

Email addresses: ongsv@vcu.edu (S. V. Ong), snkhanna@vcu.edu (S. N. Khanna)

based nanostructures. Pure graphene is a zero band gap semiconductor where the Fermi energy lies at the intersection of the filled and unfilled states and hence there is a zero density of states at the Fermi energy. For nanostructures with zigzag edges, as was pointed out by Fujita et al. [14], there is a large density of states at the Fermi energy due to states localized at the edges that can lead to a magnetic instability even for a small electron-electron interaction. The nature of the magnetic solution is driven by the symmetry of the underlying nanostructure and both ferromagnetic (FM) or antiferromagnetic (AFM) states can be stabilized by controlling the underlying nanostructure. For example, graphene can be described as a superposition of two atomic sublattices A and B. For a finite nanoribbon, the two edges are antiferromagnetically coupled if they lie on different sublattices, while they are ferromagnetically coupled if they lie on the same sublattice [4]. Geometric rules for graphene-based nanostructures including nanodots and nanoholes have also been proposed [4].

The presence of localized magnetic sites at the edges, and the ability to control their coupling by modulating the underlying lattice opens new intriguing possibilities. For example, is it possible to control the coupling of chains of magnetic elements by attaching them at the zigzag edges? More importantly, can the strength of the coupling be dependent on the physical characteristics of the underlying structure, for example the ribbon width? The purpose of this Letter is to explore this intriguing possibility by considering Fe atoms attached to the edges of zigzag carbon ribbons. Our studies, based on first principles electronic structure calculations within a gradient corrected density functional, first examine the nature of the ground state of the Fe atoms occupying edge locations. We then investigate the coupling between these chains as the width of the underlying ribbon is changed. Experimentally, it is possible to generate ribbons with edges occupied by H atoms. A comparison of the coupling between Fe or H edge atoms can then provide information if the coupling across the chains is mediated by the underlying lattice. In Section 2, we describe the theoretical approach while Section 3 presents the results and a discussion of results. Section 4 is dedicated to final conclusions.

2. Theoretical method

The theoretical studies on the zigzag ribbons decorated with Fe or H atoms were carried out within the density functional theory using the Vienna ab initio stimulation package (VASP) code [28]. The projector augmented wave (PAW) approach [29, 30] was used to describe the electron-ion interaction. The exchange correlation interactions were included through the functional proposed by Perdew et al. [31]. Brillouin zone integrations were carried out on Monkhorst-Pack k-point grids. Since the energy difference between different magnetic solutions (FM or AFM) is small, one has to be careful about the quality of the calculations to ensure the accuracy of quantitative results. To this effect, we studied the variations in the energy of both pure graphene and the Fe-terminated nanoribbon as a function of the number of k-points and as a function of the energy cut-off. For both cases, the results as a function of k-points indicated that the energy fluctuates up until 30x1x1 k-points. To have the converged results, consequently, all the nanoribbon calculations were carried out

using 35x1x1 k-points. In concurrence with testing the k-points, a study of the total energy as a function of energy cut-off showed that reasonably converged values require a kinetic energy cut-off of 450 eV for the plane wave basis. The Fe and C atom were described by using the PAW potentials [Ne] $3s^2$ $\mathbf{3p^6}$ $\mathbf{4s^2}$ $\mathbf{3d^6}$ and [He] $\mathbf{2s^2}$ $\mathbf{2p^2}$, respectively. The states shown in bold were allowed to relax. During the determination of ground state configuration, the atomic positions were optimized by moving atoms in the direction of forces till the forces were less than 10 meV/Å.

3. Results and discussion

In this work we have investigated ribbons with widths, as described by Fujita et al. [14], of N=3-10, which correspond to the edges separated by about 5-20 Å. Only zigzag terminations were included. Two complementary studies were carried out. In one case, the edge atoms were decorated with H atoms with one hydrogen atom attached to each edge C atom. In the other case, an Fe atom was attached to each carbon atom at the edge. The ground state search involved relaxing the C-C, C-H/C-Fe, and Fe-Fe bond lengths. All the calculations were carried out using a supercell that is periodic in the x-direction. Two unit cells were included in the supercell to allow for Fe-Fe interaction with a vacuum layer of ∼12 Å in the y- and z- directions to ensure no interaction between neighboring ribbons. By including two unit cells, neighboring Fe atoms were allowed to form pairs reminiscent of a Peierls distortion. Our studies indicate that such a distortion has a stabilization energy of around 200 meV per unit cell, irrespective of the ribbon width.

To assess the accuracy of the calculations, we first calculated the ground state of a free Fe_2 molecule. The geometry and the spin configuration of two Fe atoms were optimized. Our studies showed a ground state with a Fe-Fe bond length of 2.01 Å in agreement with the experimental value of 2.02 Å [32]. The calculated atomization energy of 2.77 eV is higher than the estimated experimental value of 1.14 eV [33], but is close to the previous calculated value of 2.08 eV [34]. The calculated total spin moment of $6\mu_B$ was also in agreement with previous reported values. A free Fe atom has four unpaired electrons while the Fe sites have a spin magnetic moment of $3.0\mu_B$ per atom in the ground state of Fe_2. As the Fe sites are attached to the edges, our studies indicate that the moment is reduced. An integration of the spin density around the Fe sites indicated that each Fe atom carries a moment of $2.3\mu_B$. This magnitude remains same for all widths of both AFM and FM coupled ribbon edges.

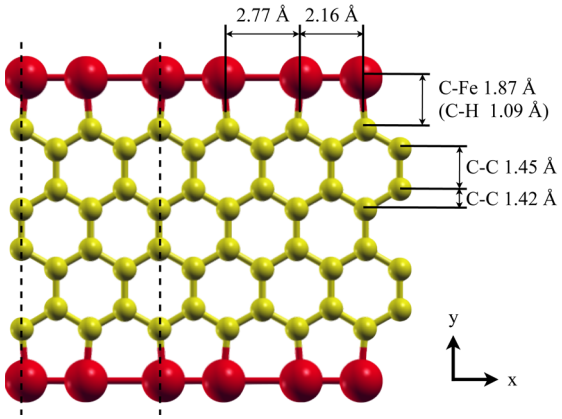

Figure 1: (Color online) Ground state geometry and bond lengths for Fe-terminated edges of a N=4 graphene nanoribbon. The large, dark (red) spheres represent iron atoms, while carbon is represented by small, lighter (yellow) spheres. Supercell width is contained between the dotted lines.

We considered the graphene ribbons with Fe atoms absorbed at the edge C sites as shown in Fig. 1. As pointed out above, the Fe-Fe distance in an isolated Fe_2 molecule is 2.01 Å while the distance between C-sites in a row is 2.46 Å. When attached to the graphene nanoribbon, the neighboring Fe atoms form pairs separated by 2.77 Å. We also examined the case where the edges were terminated by H atoms. The ground state C-C, C-H/C-Fe, and Fe-Fe separations are marked in Fig. 1.

In addition to geometry we examined the energetic stability of the ribbon decorated with Fe atoms. Note that an FeC molecule has a binding energy of 3.95 eV compared to 1.1 eV for a Fe_2 molecule indicating that FeC bonds are stronger. Our recent studies on pure Fe_n clusters containing up to eight atoms indicate that the binding energy approaches a value of 3.1 eV/atom [35]. Hence configurations where Fe sites have much higher binding energy should be stable against clustering.

An analysis of the energy required to separate Fe pairs from the edge sites using the equation

$$BE = -E_{Fe-GNR} + E_{GNR} + 4E_{Fe}, \quad (1)$$

indicates that each Fe has a binding energy of 4.23 eV. Here, E_{Fe-GNR} is the total energy calculated for the Fe terminated ribbon, E_{GNR} for the pristine ribbon, and E_{Fe} for Fe atoms. As the binding energy (4.23 eV) is higher than the energy per Fe-atom in clusters, the formation of nanoribbons decorated with Fe sites is stable against clustering of Fe-atoms. Another issue relates to the formation of Fe-decorated ribbons starting from edges with H-atoms. Considering that synthetic routes to producing graphene nanoribbons have been under a hydrogen atmosphere [8, 36], we also analyzed H_2 removal energy in H-passivated ribbons by the equation

$$BE = -E_{H-GNR} + E_{GNR} + 2E_{H_2}, \quad (2)$$

where E_{H_2} represents the total energy calculated for the H_2 molecule. The calculated energy was 2.66 eV per H atom. The corresponding calculations with formation of Fe_2 pairs showed that the pairs are more strongly bound to the C sites and favored over H_2 by 0.19 eV per atom.

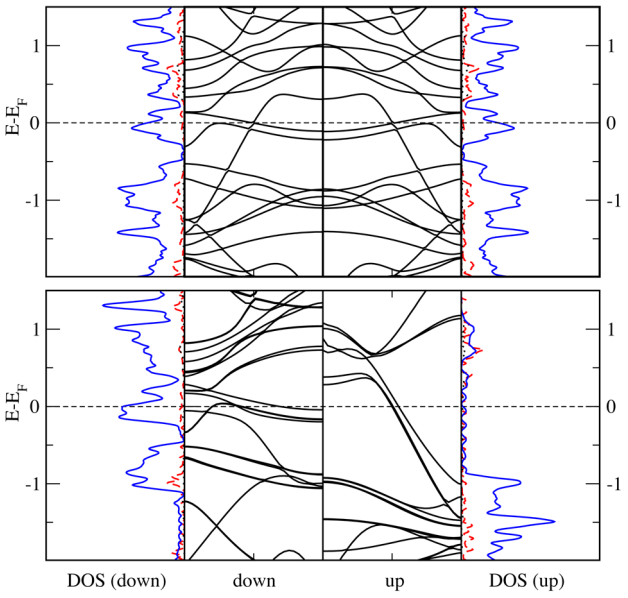

Figure 2: (Color online) Band structure for the AFM (top) and FM (bottom) configurations of the Fe-terminated zigzag edged graphene nanoribbon with width N=4. The Fermi energy (E_F) is set to zero in both plots and is highlighted with the dashed line. Extended from the bandstructure panels are the site-projected density of states for Fe d- (solid blue lines), Fe p- (dotted black lines) and C p- (dashed red lines) states.

We were particularly interested in the relative stability of the ferromagnetic and antiferromagnetic states. To this end, we calculated the energy difference between forced

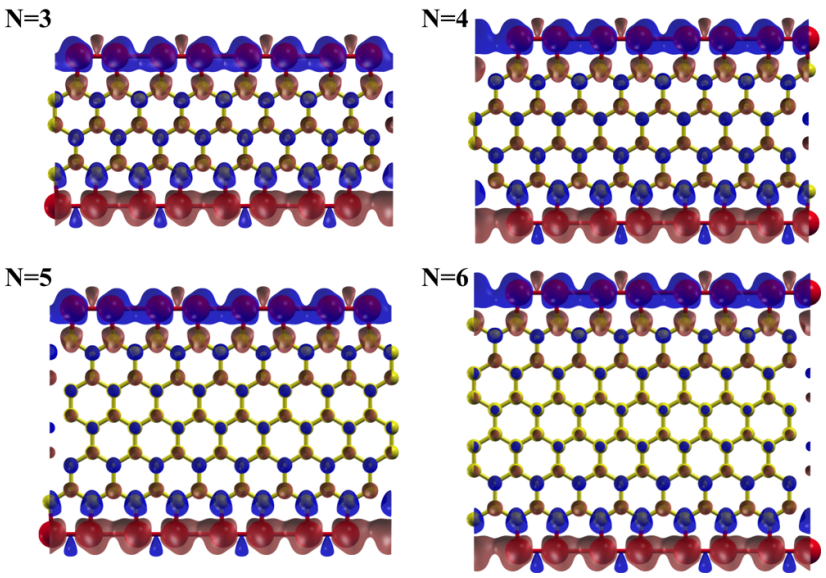

Figure 3: (Color online) Spin density figures for Fe-terminated edges of a zigzag graphene nanoribbon with widths N=3-6. An isovalue of $0.03\mu_B/\text{Å}^3$ is used. Spin-up and spin-down states are shown in dark (blue) isosurfaces and light (red) isosurfaces, respectively. Transparency is used in isosurfaces to show the large, dark (red) spheres representing Fe atoms and small, light (yellow) spheres representing C atoms.

ferromagnetic and antiferromagnetic solutions when the edges are occupied by H or by Fe atoms. For each ribbon width, our results indicate that the AFM ordering is more stable than the FM state. This is in direct agreement with the geometric rule for nanomagnetism in graphene proposed by Yu et al. [4]. Fig. 2 shows the band structure for the AFM and FM configurations, and the majority and minority spin density of states for the case of N=4. Note that there is significant density of states at the Fermi energy in both the AFM and FM case. More importantly, the states at the Fermi energy in the FM case are only composed of minority electrons. We found similar results at all ribbon widths and only results for N=4 are shown in this Letter. The finite density of states of only one spin component indicates that such a ribbon could be used to generate spin-polarized currents. This requires stabilization of the FM state and hence it is important to consider the difference in energy between the two states and its evolution with size.

Before we discuss the difference between AFM and FM solutions, let us consider how the underlying graphene stabilizes the AFM solution. We see in Fig. 3 the spin charge density for the majority and minority spin states for N=3-6. The C-sites on two sub-lattices show opposite polarization and hence help stabilize the AFM state as the Fe chains are far separated to have direct exchange interaction. The key issue is how this evolves with size. With this in mind, we show in Fig. 4, the exchange energy (difference in energy between the AFM and FM solutions) as a function of the width of the ribbon. One notices two things: (1) That the exchange energies are fairly small. Even at N=3, the difference between the

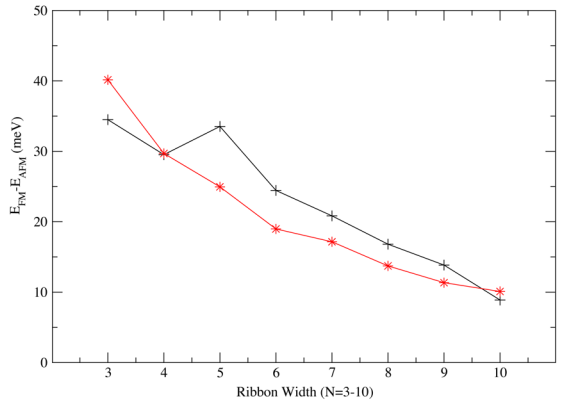

Figure 4: (Color online) Magnetic exchange energy per unit cell defined by E_{FM}-E_{AFM} shown in meV. E_{FM} is the energy of the FM ordered graphene nanoribbon, and E_{AFM} for the AFM ordered graphene nanoribbon. The dark (black) plus symbols corresponds to the ribbons with Fe-terminated edges, where the light (red) asterisk symbols corresponds to the ribbons with H-terminated edges. The lines are shown as guides.

AFM and FM solution is only around 35 meV. Since the ground state is AFM, this shows that the FM state could be stabilized by applying magnetic fields. (2) The exchange interaction decreases as a function of the width. Since one does not expect significant direct exchange coupling between Fe-chains, this indicates that as the width is increased, the ribbon becomes softer to stabilize the AFM solution. To further show that this effect is intrinsic to the ribbon and not related to Fe atoms, we calculated the energy difference between the AFM and FM solutions by replacing Fe atoms by H atoms. The corresponding results are shown in Fig. 4 and the values are close to those for Fe, indicating that the effect is intrinsic to the graphene nanoribbon.

4. Conclusions

Our studies indicate that the zigzag graphene ribbons decorated with Fe atoms at the edges have a ground state where the Fe-atoms form dimers. The chains at the two ends of the ribbon are coupled anti-ferromagnetically where the coupling is mediated by the spin-orbitals localized at the two sub-lattices. The difference between the AFM and FM solution, however decreases with increasing width and is only around 9 meV for ribbons with N=10. The small energy difference could be overcome by applying magnetic field that should stabilize the FM state. As the states at the Fermi energy in FM solution are primarily minority in character, it may be possible to have spin-polarized currents in such ribbons.

The authors also acknowledge support from US Department of the Army through a MURI Grant # W911NF-06-1-0280.

References

[1] K. S. Novoselov, A. K. Geim, S. V. Morozov, D. Jiang, Y. Zhang, S. V. Dubonos, I. V. Grigorieva, A. A. Firsov, Science 306 (2004) 666–669.

[2] K. S. Novoselov, Proceedings of the National Academy of Sciences 102 (2005) 10451–10453.

[3] A. K. Geim, K. S. Novoselov, Nature Materials 6 (2007) 183–191.

[4] D. Yu, E. Lupton, H. Gao, C. Zhang, F. Liu, Nano Research 1 (2008) 497–501.

[5] A. C. Neto, F. Guinea, N. Peres, K. Novoselov, A. Geim, Reviews of Modern Physics 81 (2009) 109–162.

[6] Y. Zhang, Y. Tan, H. L. Stormer, P. Kim, Nature 438 (2005) 201–204.

[7] K. S. Novoselov, A. K. Geim, S. V. Morozov, D. Jiang, M. I. Katsnelson, I. V. Grigorieva, S. V. Dubonos, A. A. Firsov, Nature 438 (2005) 197–200.

[8] Y. Kobayashi, K. Fukui, T. Enoki, K. Kusakabe, Physical Review B 73 (2006).
[9] M. Y. Han, B. Özyilmaz, Y. Zhang, P. Kim, Physical Review Letters 98 (2007) 206805–4.
[10] K. A. Ritter, J. W. Lyding, Nature Materials 8 (2009) 235–242.
[11] C. Girit, J. Meyer, R. Erni, M. Rossell, C. Kisielowski, L. Yang, C. Park, M. Crommie, M. Cohen, S. Louie, A. Zettl, Science 323 (2009) 1705–1708.
[12] X. Jia, M. Hofmann, V. Meunier, B. G. Sumpter, J. Campos-Delgado, J. M. Romo-Herrera, H. Son, Y. Hsieh, A. Reina, J. Kong, M. Terrones, M. S. Dresselhaus, Science 323 (2009) 1701–1705.
[13] M. Terrones, Nature 458 (2009) 845–846.
[14] M. Fujita, K. Wakabayashi, K. Nakada, K. Kusakabe, Journal of the Physical Society of Japan 65 (1996) 1920–1923.
[15] K. Nakada, M. Fujita, G. Dresselhaus, M. S. Dresselhaus, Physical Review B 54 (1996) 17954.
[16] D. Jiang, B. G. Sumpter, S. Dai, The Journal of Chemical Physics 126 (2007) 134701.
[17] F. Schedin, A. K. Geim, S. V. Morozov, E. W. Hill, P. Blake, M. I. Katsnelson, K. S. Novoselov, Nature Materials 6 (2007) 652–655.
[18] J. Fernández-Rossier, J. Palacios, Physical Review Letters 99 (2007).
[19] T. Wassmann, A. P. Seitsonen, A. M. Saitta, M. Lazzeri, F. Mauri, Physical Review Letters 101 (2008) 096402–4.
[20] H. Sevinçli, M. Topsakal, E. Durgun, S. Ciraci, Physical Review B 77 (2008) 195434–7.
[21] A. V. Krasheninnikov, P. O. Lehtinen, A. S. Foster, P. Pyykko, R. M. Nieminen, Physical Review Letters 102 (2009) 126807–4.
[22] D. Jiang, X. Q. Chen, W. Luo, W. Shelton, Chemical Physics Letters 483 (2009) 120–123.
[23] V. Barone, O. Hod, G. E. Scuseria, Nano Letters 6 (2006) 2748–2754.
[24] Y. Son, M. L. Cohen, S. G. Louie, Nature 444 (2006) 347–349.
[25] Y. Son, M. L. Cohen, S. G. Louie, Physical Review Letters 97 (2006) 216803–4.
[26] L. Pisani, J. A. Chan, B. Montanari, N. M. Harrison, Physical Review B 75 (2007) 064418–9.
[27] P. Esquinazi, A. Setzer, R. Höhne, C. Semmelhack, Y. Kopelevich, D. Spemann, T. Butz, B. Kohlstrunk, M. Lösche, Physical Review B 66 (2002) 024429.
[28] G. Kresse, J. Furthmüller, Computational Materials Science 6 (1996) 15–50.
[29] P. Blöchl, Physical Review B 50 (1994) 17953–17979.
[30] G. Kresse, D. Joubert, Physical Review B 59 (1999) 1758–1775.
[31] J. Perdew, K. Burke, M. Ernzerhof, Physical Review Letters 77 (1996) 3865–3868.
[32] H. Purdum, P. Montano, G. Shenoy, T. Morrison, Physical Review B 25 (1982) 4412–4417.
[33] L. Lian, C. Su, P. B. Armentrout, The Journal of Chemical Physics 97 (1992) 4072–4083.
[34] M. Castro, C. Jamorski, D. R. Salahub, Chemical Physics Letters 271 (1997) 133–142.
[35] D. R. Roy, R. Robles, S. N. Khanna, [Unpublished Work] (2010).
[36] Z. Klusek, Z. Waqar, E. A. Denisov T. N. Kompaniets, I. V. Makarenko, A. N. Titkov, A. S. Bhatti, Applied Surface Science 161 (2000) 508–514.